Analytical and practical analysis of frictional-kinetic model for dense and dilute gas-solid flows

Pascal Fede, François Audard, Emmanuel Belut, Jean-Raymond Fontaine, Olivier Simonin

Analytical and practical analysis of frictional-kinetic model for dense and dilute gas-solid flows

Pascal Fede[1], François Audard[1], Emmanuel Belut[2], Jean-Raymond Fontaine[2], Olivier Simonin[1]

[1] *Institut de Mécanique des Fluides de Toulouse (IMFT), Université de Toulouse, CNRS, INPT, UPS, FR-31400 Toulouse FRANCE*
[2] *INRS - Laboratoire d'Ingénierie Aéraulique, FR-54500 Vandœuvre, France*

Abstract

In granular flows, when the solid volume fraction is large, the dynamic behaviour of particles becomes controlled by frictional effects. Theoretically these effects can not be taken into account in an Eulerian approach, based on the kinetic theory of granular flows, because the inter-particle contact times are long. However, in the literature several empirical models have been proposed which introduce a frictional pressure and viscosity. In the paper, these models are first compared on a simple case of sheared dense granular flows in order to analyze the individual behavior of each model. Second, the models have been implemented in an Eulerian solver and numerical simulations have been performed of an experiment of bin discharge [3]. The results show that for large diameter, the solid mass flow rate is well predicted, while it is systematically underestimated when the ratio between the injector diameter and the diameter of particles is small.

Keywords: Frictional viscosity ; Multi-fluid model ; Granular flow

1. Introduction

Granular flows are encountered in many practical applications such as fluidized beds in chemical process (Fluid Catalytic Cracking, polypropylene production), production of electricity (circulating fluidized bed combustion, pyrolysis of biomass), powder handling (silo discharge, pneumatic conveying), or geophysical flows (sand dune motion, ripple formation, volcano eruption). In these applications the granular flows exhibit different regimes which can be sorted according to the particle volume fraction, α_p. In dilute flows ($\alpha_p < 0.01\%$), the particle motion is mainly controlled by the interaction with the turbulence. A kinetic regime can be defined for $0.01\% < \alpha_p < 10\%$. In such a regime the solid phase transport properties is due to the particle fluctuating (random or turbulent) velocity with a mixing length scale controlled by inter-particle collisions and/or fluid-particle interactions. The two-way coupling (i.e. the modification of the fluid flow by the particle) may be present if the particle mass loading is sufficiently large. Finally for $\alpha_p > 10\%$ takes place a dense gas-particle regime with two sub-regimes:

- Rapid granular flows (short inter-particle contact time) or collisional regime: solid phase transport properties due to inter-particle exchanges by collision (negligible effect of the interstitial gas).
- Slow granular flows (long inter-particle contact time) or frictional regime: solid phase rheology due to inter-particle friction.

Basically, the numerical simulation of granular flows can be performed in a Lagrangian or an Eulerian way. However the Lagrangian approach can not be used for a practical application because of the huge number of particles that must be tracked. In contrast, an Eulerian approach is much more adapted for complex and large-scale geometries but the Eulerian approach needs closures law for inter-particle collisions and high-order terms.

Eulerian approaches are based on the kinetic theory of granular flow (KTGF) [14, 4, 19] with additional terms taking into account the effects of interstitial fluid. From a theoretical point of view, such an approach is valid for dilute regime and also dense regime but only for the sub-regime called "Rapid granular flows" because the KTGF is based on the idea that the inter-particle collision are instantaneous. The present paper focuses on the modelling of "Slow granular flow" in the frame of Eulerian approach. In the following section several models from the literature are introduced. These models are compared on a simple case of sheared granular flows in order to understand the main differences between the models. Finally the predictions of the models are compared with experimental data for the case of a bin discharge [3].

2. Gas-particle mathematical model

The mathematical model is given in appendix. All details of the mathematical model can be found in [4, 19, 6]. The momentum equation of the particle phase reads

$$\begin{aligned}\alpha_p\rho_p\left[\frac{\partial U_{p,i}}{\partial t}+U_{p,j}\frac{\partial U_{p,i}}{\partial x_j}\right] = & - \alpha_p\frac{\partial P_g}{\partial x_i} \\ & + \alpha_p\rho_p g_i \\ & + I_{g\to p,i} \\ & - \frac{\partial}{\partial x_j}\left[\Sigma^{coll}_{p,ij}+\Sigma^{fr}_{p,ij}\right]\end{aligned} \quad (1)$$

where, ρ_p is particle density, $U_{p,i}$ is the i^{th}-component of the mean velocity, P_g the mean gas pressure, and g_i is the gravity. The third term on the right-hand-side is the mean gas-particle momentum transfer.

$$\begin{aligned}\alpha_p\rho_p\left[\frac{\partial q_p^2}{\partial t}+U_{p,j}\frac{\partial q_p^2}{\partial x_j}\right] = & \\ & - \frac{\partial}{\partial x_j}\left[\alpha_p\rho_p\left(K_p^{kin}+K_p^{col}\right)\frac{\partial q_p^2}{\partial x_j}\right] \\ & - \Sigma^{coll}_{p,ij}\frac{\partial U_{p,i}}{\partial x_j} \\ & - \frac{\alpha_p\rho_p}{\tau^F_{gp}}\left(2q_p^2-q_{gp}\right) \\ & - \alpha_p\rho_p\frac{1}{3}\frac{1-e_c^2}{\tau_c}q_p^2.\end{aligned} \quad (2)$$

The transport equations are derived by phase ensemble averaging for the continuous phase and in the frame of kinetic theory

of granular flows [14] for the dispersed phase but extended to account for interstitial fluid effects and particle-turbulence interaction [2]. The fluid-particle momentum transfers are taken into account by the model proposed by [9]. The turbulence of the gas phase is computed using the $k-\epsilon$ model, and particle agitation is treated by the $q_p^2 - q_{gp}^p$ model. It is assumed that the particle agitation is purely decorrelated [20]. In fact these hypotheses are legitimate due to inertia of particle. The complete description of the mathematical model can be found in [4, 9, 19]. As explained in introduction, the particulate flow regime passes from quasi-staic to dilute flows. Then the frictional effects have to be taken into account in the modelling approach, especially in the silo.

In the present study, a frictional contribution has been added to the particle kinetic stress tensor in the momentum equation. The model for frictional effects has been proposed by Johnson and Jackson [11] for the pressure and Srivastava and Sundaresan [21] for the viscosity. Frictional effects are assumed to be directly dissipated into heat without affecting the agitation. The frictional contribution doesn't appear in the particle agitation equation, in particular the friction effect has been neglected.

3. Model for frictional effects

In the present section several models for taking into account the frictional effect are introduced. These models are essentially extensions of soil mechanics [17]. Basically, the frictional stress tensor, $\Sigma_{p,ij}^{fr}$, is given in term of fritional pressure, P_{fr}, viscosity, μ_{fr} as

$$\Sigma_{p,ij}^{fr} = P_{fr}\delta_{ij} - 2\mu_{fr}\tilde{D}_{p,ij} \tag{3}$$

where $\tilde{D}_{p,ij}$ is the strain rate tensor given in the appendix.

3.1. Johnson & Jackson model (1990) [11]

Johnson & Jackson [11] proposed the following model for the frictional pressure

$$P_{fr}^{JJ} = \begin{cases} Fr\frac{(\alpha_p-\alpha_p^{\min})^r}{(\alpha_p^{\max}-\alpha_p)^s} & \text{if} \quad \alpha_p > \alpha_p^{\min} \\ 0 \quad \text{otherwise} \end{cases} \tag{4}$$

where Fr, r and s are empirical material constants. For glass beads these constants can be chosen such as $Fr = 0.05$, $r = 2$, $s = 5$ and the threshold particle volume fraction $\alpha_p^{\min}$ is set to 0.5.

3.2. Srivastava & Sundaresan (2003) (SS model)[21]

At the critical state the granular material deforms without any volume change ($\nabla \cdot \mathbf{U}_p = 0$), Srivastava & Sundaresan [21] proposed to model the frictional viscosities as

$$\mu_{fr}^{SS} = \begin{cases} \frac{\sqrt{2}P_{fr}^{JJ}\sin(\phi)}{2\sqrt{\underline{\underline{\tilde{D}_p}}:\underline{\underline{\tilde{D}_p}}+\frac{2}{3}\frac{q_p^2}{d_p^2}}} & \text{if} \quad \alpha_p > \alpha_p^{\min} \\ 0 \quad \text{otherwise} \end{cases} \tag{5}$$

where ϕ is the angle of internal friction, set to 28.5°.

3.3. Schneiderbauer et al. (2012) (SAP model) [18]

In 2012, Schneiderbauer et al. [18] proposed a model for the frictional pressure and viscosity based on the $\mu(I)$-rheology. The granular pressure reads

$$P_{fr}^{SAP} = 4\rho_p \frac{\left(bd_p\sqrt{\underline{\underline{D_p}}:\underline{\underline{D_p}}}\right)^2}{\left(\alpha_p^{max}-\alpha_p\right)^2} \tag{6}$$

where$b \approx 0.2$ is a model constants [8]. The frictional viscosity is given by

$$\mu_{fr}^{SAP} = \frac{P_{fr}^{SAP}}{2\sqrt{\underline{\underline{D_p}}:\underline{\underline{D_p}}}}\,\mu_i(I) \tag{7}$$

where $\mu_i(I)$ is a function. From experiments, Jop et al. (2006) [12] proposed

$$\mu_i(I) = \mu_i^{st} + \frac{\mu_i^c - \mu_i^{st}}{I_0/I_s + 1} \tag{8}$$

with $I_0 = 0.279$, $\mu_i^{st} = 0.382$ and $\mu_i^c = 0.6435$. In Eq.,(8), I_s is the inertial number that is computed by:

$$I_s = \frac{2\sqrt{\underline{\underline{D_p}}:\underline{\underline{D_p}}}d_p}{\sqrt{P_{fr}^{SAP}/\rho_p}}. \tag{9}$$

4. Simple sheared granular flows

This section is dedicated to the analysis of the frictional models on a simple configuration of sheared granular flows. In such a configuration only the equation of the particle agitation Eq. (2) has been solved. The production by the mean shear is balanced by the dissipation due to non-elastic inter-particle collisions. The gas is air with a density of $\rho_f = 1.224\,\mathrm{kg/m^3}$ and a viscosity of $\mu_f = 1.78 \cdot 10^{-5}\,\mathrm{kg/m/s}$. The particle density is set to $\rho_p = 2500\,\mathrm{kg/m^3}$ and the particle diameter is $d_p = 487\,\mu\mathrm{m}$.

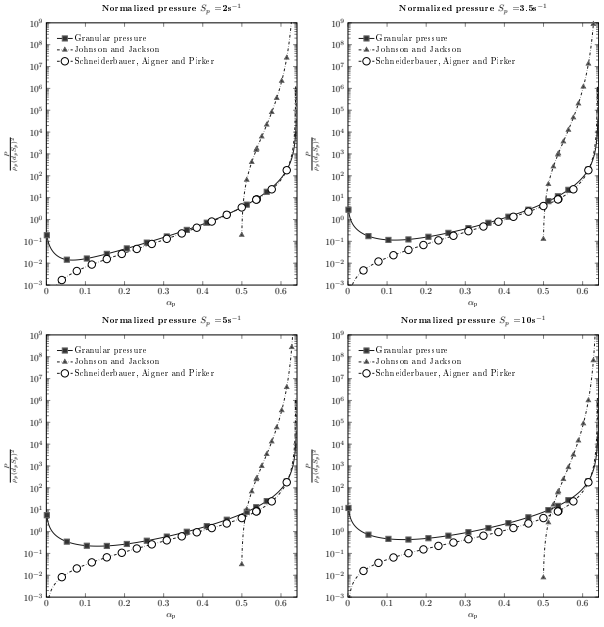

Figure 1: Normalized pressure by $\rho_p(d_pS_p)^2$ with respect to the particle volume fraction α_p for several values of the mean shear S_p.

Figures 1 and 2 shows the normalized pressure and normalized viscosity with respect to the particle volume fraction for different value shear stress (S_p). For low volume fractions, the flow is lead by the competition between the collisions and fluid flow. This regime corresponds to the kinetic one. When the volume fraction increases a transition to the collisional regime is observed. For higher volume fraction the frictional pressure and viscosity is increased. This comes from the long long contact times and the frictional interaction between particles. The

Johnson and Jackson frictional pressure model [11] presents a rapid transition from the dilute to the dense regime. This passage will take place after the threshold particle volume fraction. One may note that the pressure in Schneiderbauer et al.'s model [18] corresponds to the intermediate pressure proposed by [5], without the quasi-static contribution. The intermediate pressure links the dilute and dense regimes. Adding the frictional contribution proposed by [18] shows a smooth transition from the kinetic-collisional regime to the frictional regime. As will be seen below, the SAP model [18] allows a smoother transition to the frictional regime.

The granular and frictional pressures are shown by Figure 1. As expected the frictional pressure acts at large solid volume fractions.

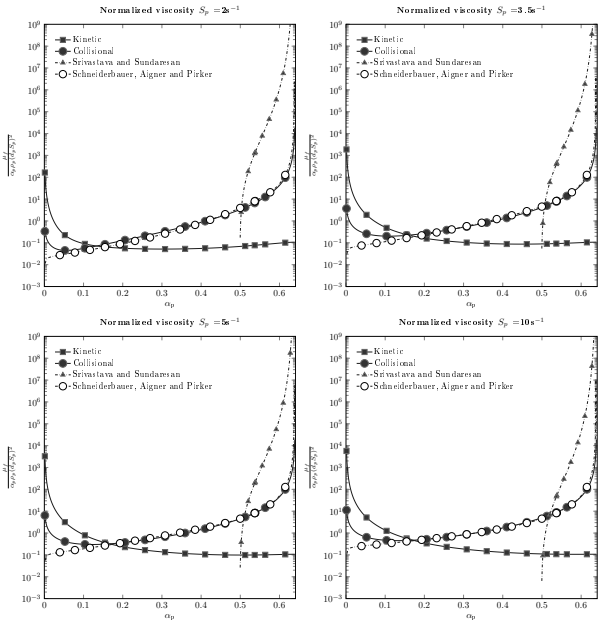

Figure 2: Normalized viscosity by $\alpha_p \rho_p (d_p S_p)^2 / S_p$ with respect to the particle volume fraction α_p for several values of th mean shear S_p.

5. Simulations and experiments

In this section, numerical simulations of a silo discharge are performed. The modelling of the frictional term is performed with the data base given by [3]. Figure 3 shows the experimental geometry.The geometry consists of a rectangular bin 60 mm x 3.5 mm and x 500 mm height. The mesh contains 25000 hexahedral cells with a grid resolution of $\Delta x \sim 1$ mm, Δy = 0.875 mm and Δz = 3.125 mm. A region below the bin (0.1m) has been added which allows the granular media to pass through the orifice. Computations on a refined mesh have been performed and showed no sensitivity on the results. The different meshes are not shown in this paper. The particles are glass beads of density ρ_p = 2500 kg/m^3. Different particle diameters have been considered and are summarized in table 1. The air characteristics are the same as those of the previous section.

Table 1: Monodisperse data base made by [3] on rectangular configuration $L \cdot W \cdot H = 0.06 \cdot 0.0035 \cdot 0.5$m. Tbe bin outlet has length $D = 0.00739$ m, and a thickness $W = 0.0035$.

D/d_p	$Q \cdot 10^3 (kg/s)$	$v_f \cdot 10^2 (m/s)$	$\phi(-)$
64.825	9.4	3.014	0.594
64.825	9.3	2.932	0.594
36.049	9.2	2.959	0.592
36.049	9.1	2.850	0.592
22.394	8.1	2.598	0.582
22.394	7.9	2.521	0.582
15.175	7.8	2.336	0.616
15.175	7.9	2.399	0.616
10.264	7.1	2.514	0.607
6.837	4.9	1.617	0.573
6.837	4.9	1.539	0.573
5.685	4.5	1.537	0.605
5.685	4.5	1.687	0.605

The author [10] find a good agreement for the particle mass flow rate (Q) with beverloo's law expressed in this form, for a rectangular configuration:

$$Q = C\rho\phi\sqrt{g}W(D - kd_p)^{3/2}. \tag{10}$$

with the coefficient found $C = 0.91$ et $k = 1.36$.

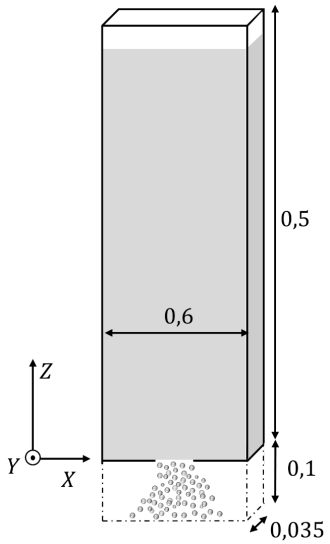

Figure 3: Bin discharge geometry based on [3].

Three dimensional numerical simulations has been performed using an Eulerian multi-fluid modelling approach for gas and solid interaction developed and implemented by IMFT (Institut de Mécanique des Fluides de Toulouse) in the NEPTUNE_CFD. NEPTUNE_CFD is a multiphase flow software developed in the framework of the NEPTUNE project, financially supported by CEA (Commissariat à l'Energie Atomique), EDF (Electricité de France), IRSN (Institut de Radioprotection et de Sûreté Nucléaire) and AREVA-NP. The numerical solver has been developed for High Performance Computing [16, 15]. Each numerical simulation has been performed for 10 seconds and time-averaged statistics are computed during the last 6 seconds. Test performed with and without turbulence gas model, and no significant effect was observed.

6. Comparisons

Figure 4 shows the temporal mass flow rate evolution for the different frictional models. Stabilization of the mass flow rate around the mean values takes 4 seconds for all numerical simulations. Small fluctuations have been observed around a mean value. Table 6 shows the results with the different frictional models described in section 3. For each simulation an underestimation of the mean flow rate is observed. The figure 5 compares the experimental and Beverloo law to the numerically predicted dimensionless mass flow rate. A good shape is predicted and the model better captures the mass flow rate for high D/d_p ratios. The results with the SS model show a better agreement with the experimental value. In contrast the frictional models have some difficulty to correctly predict the particle mass flow rate when D/d_p is small.

The simulation with the SS model, high fluctuations for low particle diameters have been observed (see Figure 6). This is provoked by the penetration of air into the system. These fluctuations help the mixing at the injector and create more shearing and agitation. This can reduce the effect of frictional viscosity.

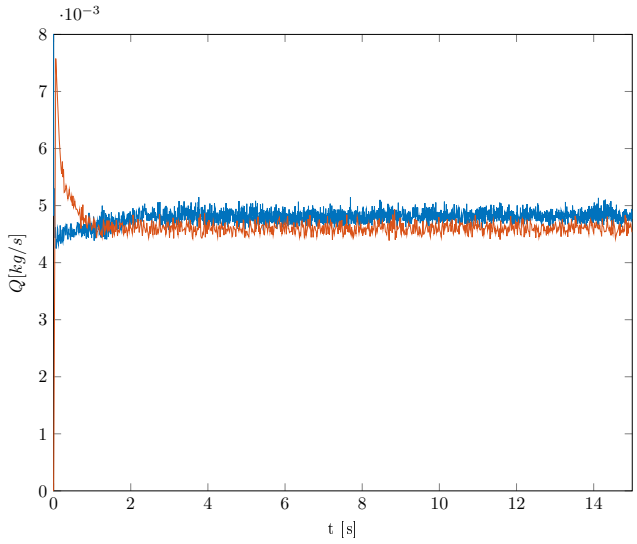

Figure 4: Temporal evolution of the solid mass flow rate for a particle diameter $d_p = 487\mu$m. Blue line represent the SS model [21], and the red line represent the [18] model.

Table 2: Time-averaged particle mass flow rates (in gr.s^{-1}) measured in numerical simulations, e represent the relative error ($[Q_{sim} - Q_{exp}]/Q_{sim}$) in %.

D/d_p	Exp.	SS model	e_{SS}	SAP model	e_{SAP}
64.82	9.4	7.91	15.85	6.53	30.53
36.04	9.2	7.53	18.15	6.47	29.67
22.39	8.1	6.09	24.81	5.61	30.74
15.17	7.8	4.80	38.46	4.60	41.02
10.26	7.1	3.77	46.90	3.66	48.45
6.83	4.9	2.80	42.85	2.79	43.06
5.68	4.5	2.64	41.33	2.46	45.33

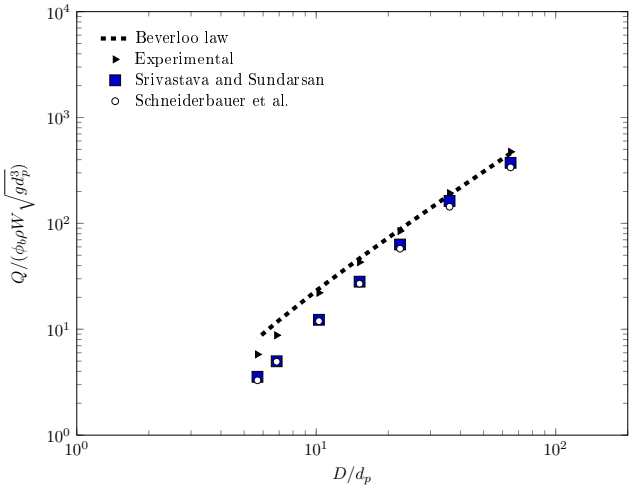

Figure 5: Dimensionless mass flow rate $Q/\rho\phi_b W\sqrt{gd_p^3}$. Dash line represent the Beverloo law eq. 10, symbol represent the experimental value given by [3], and numerical simulation with the different correlation show in section 3

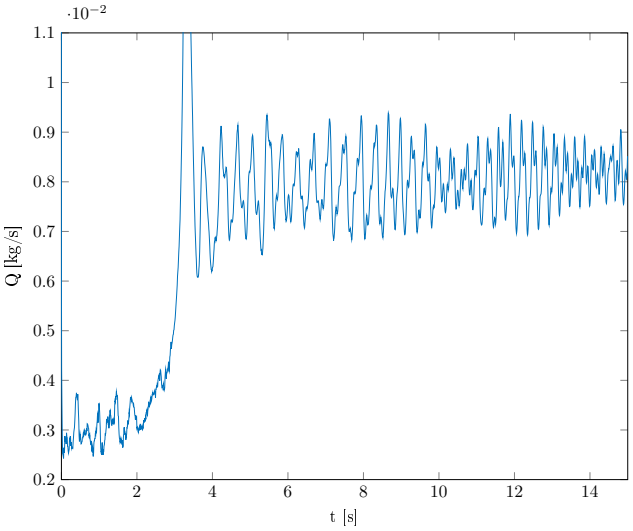

Figure 6: Temporal evolution of the particle mass flow rate for the SS model [21].

7 shows the velocity profile at the injector for the different diameters, for the case with the SS model and JJ model. Free fall arch hypothesis near to the injector suggests that particles fall like a solid in vacuum ($\sqrt{gD}$). When we compare the mean particle velocity to the numerical results a good agreement is obtained for hight D/d_p ratio. However when this ratio is reduced the particle mean velocity decreases.

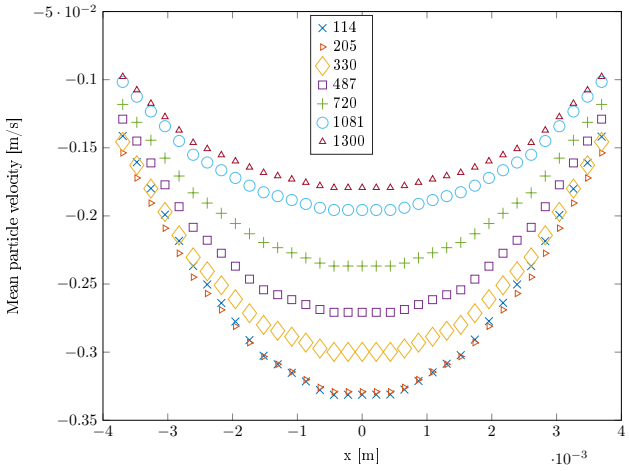

Figure 7: Mean particle velocity profiles at the injector (centered on the middle) with the Sundaresan & Srivastava model, for different particle diameter.

7. Conclusion

The results show that the frictional viscosity model captures the shape of the beverloo law. A better agreement to the experimental value has been found for the particle mass flow rate at high D/d_p ratio. As for the high ratio the velocity follows the free fall arch assumption, the velocity fall like particle in vacuum. When the ratio becomes low (corresponding to only a few particles passing through the bin outlet orifice) the different models have some difficulty to correctly predict the mass flow rate. Moreover recent development on rotating drum show an underestimation of the slope of the particle bed free surface. For the Srivastava & Sundaresan model, some numerical simulations (not shown) suggest this underestimation could be due to the q_p^2 term (see equation 5) in the frictional viscosity. Frictional effects do not explicitly appear in the kinetic agitation equation and only appear through the effect on the momentum equation. As a matter of fact, frictional effects should induced an additional dissipation of the random kinetic energy which is not accounted for in the actual modelling approach and required further investigations. In recent development by Chialvo & et al. propose to consider an intermediate and quasi-static transition. This is under consideration in forthcoming work.

References

[1] G. Balzer. Gas-solid flow modelling based on the kinetic theory of granular media: validation, applications and limitations. *Powder Technology*, 113:299 – 309, 2000.

[2] G. Balzer, A. Boëlle, and O. Simonin. Eulerian gas-solid flow modeling of dense fluidized bed. In *FLUIDIZATION VII, Proc International Symposium of the Engineering Foundation*, pages 1125–1134, 1995.

[3] M Benyamine, M Djermane, B Dalloz-Dubrujeaud, and P Aussillous. Discharge flow of a bidisperse granular media from a silo. *Physical Review E*, 90(3):032201, 2014.

[4] A. Boëlle, G. Balzer, and O. Simonin. Second-order prediction of the particle-phase stress tensor of inelastic spheres in simple shear dense suspensions. In *Gas-Particle Flows*, volume 228, pages 9 – 18. ASME FED, 1995.

[5] S. Chialvo, J. Sun, and S. Sundaresan. Bridging the rheology of granular flows in three regimes. *Physical Review E*, 85(2):021305, 2012.

[6] P. Fede, O. Simonin, and A. Ingram. 3D numerical simulation of a lab-scale pressurized dense fluidized bed focussing on the effect of the particle-particle restitution coefficient and particle–wall boundary conditions. *Chemical Engineering Science*, 142:215–235, 2016.

[7] G. Ferschneider and P. Mège. Dilute gas-solid flow in a riser. *Chemical Engineering Journal*, 87:41 – 48, 2002.

[8] Y. Forterre and O. Pouliquen. Flows of dense granular media. *Annu. Rev. Fluid Mech.*, 40:1–24, 2008.

[9] A. Gobin, H. Neau, O. Simonin, J. R. Llinas, V. Reiling, and J. L. Sélo. Fluid dynamic numerical simulation of a gas phase polymerisation reactor. *International Journal for Numerical Methods in Fluids*, 43:1199–1220, 2003.

[10] A Janda, Iker Zuriguel, A Garcimartin, Luis A Pugnaloni, and Diego Maza. Jamming and critical outlet size in the discharge of a two-dimensional silo. *EPL (Europhysics Letters)*, 84(4):44002, 2008.

[11] P.C. Johnson, P. Nott, and R. Jackson. Frictional–collisional equations of motion for participate flows and their application to chutes. *Journal of Fluid Mechanics*, 210:501–535, 1990.

[12] P. Jop, Y. Forterre, and O. Pouliquen. A constitutive law for dense granular flows. *Nature*, 441(7094):727–730, 2006.

[13] C.K.K. Lun and S.B. Savage. The effetcs of an impact velocity dependent coefficient of restitution on stresses developed by sheared granular materials. *Acta Mechanica*, 63:539–559, 1986.

[14] C.K.K. Lun, S.B. Savage, D.J. Jeffrey, and N. Chepurniy. Kinetic theories for granular flow : inelastic particles in couette flow and slightly inelastic particles in a general flowflied. *J. Fluid Mech.*, 140:223–256, 1984.

[15] H. Neau, P. Fede, J. Laviéville, and O. Simonin. High performance computing (hpc) for the fluidization of particle-laden reactive flows. In *The 14th International Conference on Fluidization - From Fundamentals to Products*, 2013.

[16] H. Neau, J. Laviéville, and O. Simonin. NEPTUNE_CFD high parallel computing performances for particle-laden reactive flows. In *7th International Conference on Multiphase Flow, ICMF 2010, Tampa, FL, May 30 - June 4*, 2010.

[17] D.G. Schaeffer. Instability in the evolution equations describing incompressible granular flow. *Journal of differential equations*, 66(1):19–50, 1987.

[18] S. Schneiderbauer, A. Aigner, and S. Pirker. A comprehensive frictional-kinetic model for gas–particle flows: Analysis of fluidized and moving bed regimes. *Chemical Engineering Science*, 80:279–292, 2012.

[19] O. Simonin. Combustion and turbulence in two-phase flows. In *Lecture Series 1996-02*. Von Karman Institute for Fluid Dynamics, 1996.

[20] O. Simonin, P. Février, and J. Laviéville. On the spatial distribution of heavy particle velocities in turbulent flow : From continuous field to particulate chaos. *Journal of Turbulence*, 3(040):1 – 18, 2002.

[21] A. Srivastava and S. Sundaresan. Analysis of a frictional-kinetic model for gas-particle flow. *Powder Technology*, 129:72–85, 2003.

A. Appendix: Mathematical model

In the following when subscript $k = g$ we refer to the gas and $k = p$ to the particulate phase. The mass balance equation (without interphase mass transfer) is written

$$\frac{\partial}{\partial t}\alpha_k\rho_k + \frac{\partial}{\partial x_j}\alpha_k\rho_k U_{k,j} = 0$$

where α_k is the volume fraction of the phase k, ρ_k the material density and $U_{k,i}$ the i^{th} component of the k-phase mean velocity.

The mean momentum transport equation is written

$$\begin{aligned}\alpha_k\rho_k\left[\frac{\partial}{\partial t} + U_{k,j}\frac{\partial}{\partial x_j}\right]U_{k,i} = &- \alpha_k\frac{\partial P_g}{\partial x_i}\\ &+ \alpha_k\rho_k g_i\\ &+ I_{k,i}\\ &- \frac{\partial\Sigma_{k,ij}}{\partial x_j}\end{aligned}$$

where P_g is the mean gas pressure, g_i the gravity acceleration, $\Sigma_{k,ij}$ the effective stress tensor, and $I_{k,i}$ the mean gas-particle interphase momentum transfer without the mean gas pressure contribution. According to the large particle to gas density ratio, only the drag force is acting on the particles. The mean gas-particle interphase momentum transfer term is written as:

$$I_{p,i} = -\alpha_p\rho_p\frac{V_{r,i}}{\tau^F_{gp}} \quad \text{and} \quad I_{g,i} = -I_{p,i}.$$

The particle relaxation time scale is written

$$\frac{1}{\tau^F_{gp}} = \frac{3}{4}\frac{\rho_g}{\rho_p}\frac{\langle|\mathbf{v}_r|\rangle}{d_p}C_d$$

where C_d is the drag coefficient given by [9]. The mean fluid-particle relative velocity, $V_{r,i}$, is given in terms of the mean gas and solid velocities: $V_{r,i} = U_{p,i} - U_{f,i} + V_{d,i}$. With $V_{d,i}$ is the turbulent gas-particle drift velocity without the subgrid effect. The solid stress tensor is written

$$\Sigma^{coll}_{p,ij} = \alpha_p\rho_p\left\langle u'_{p,i}u'_{p,j}\right\rangle + \Theta_{p,ij}$$

where $u'_{p,i}$ is the fluctuating part of the instantaneous solid velocity and $\Theta_{p,ij}$ the collisional particle stress tensor. The solid stress tensor is expressed as [4, 7, 1],

$$\Sigma^{coll}_{p,ij} = \left[P_p - \lambda_p D_{p,mm}\right]\delta_{ij} - 2\mu_p\tilde{D}_{p,ij}$$

where the strain rate tensor is defined by

$$\tilde{D}_{p,ij} = D_{p,ij} - \frac{1}{3}D_{p,mm}\delta_{ij} \quad \text{with} \quad D_{p,ij} = \frac{1}{2}\left[\frac{\partial U_{p,i}}{\partial x_j} + \frac{\partial U_{p,j}}{\partial x_i}\right]$$

The granular pressure, viscosities and model coefficients are given by

$$\begin{aligned}P_p &= \frac{2}{3}\alpha_p\rho_p q_p^2\left[1 + 2\alpha_p g_0(1+e_c)\right]\\ \lambda_p &= \frac{4}{3}\alpha_p^2\rho_p d_p g_0(1+e_c)\sqrt{\frac{2}{3}\frac{q_p^2}{\pi}}\\ \mu_p &= \alpha_p\rho_p\left(\nu_p^{kin} + \nu_p^{col}\right)\\ \nu_p^{kin} &= \left[\frac{1}{3}q_{gp}\tau^t_{gp} + \frac{1}{2}\tau^F_{gp}\frac{2}{3}q_p^2(1+\alpha_p g_0\zeta)\right] / \left[1 + \frac{\sigma}{2}\frac{\tau^F_{gp}}{\tau_c}\right]\\ \nu_p^{col} &= \frac{4}{5}\alpha_p g_0(1+e_c)\left[\nu_p^{kin} + d_p\sqrt{\frac{2}{3}\frac{q_p^2}{\pi}}\right]\\ \zeta &= \frac{2}{5}(1+e_c)(3e_c-1)\\ \sigma &= \frac{1}{5}(1+e_c)(3-e_c).\end{aligned}$$

Decorrelated collision model is used, the collision time scale τ_c is given by

$$\frac{1}{\tau_c} = 4\pi g_0 n_p d_p^2\sqrt{\frac{2}{3\pi}q_p^2}$$

where the radial distribution function, g_0, is computed according to [13] as

$$g_0(\alpha_p) = \left[1 - \frac{\alpha_p}{\alpha_{max}}\right]^{-2.5\alpha_{max}}$$

where $\alpha_{max} = 0.64$ is the closest random packing.

The solid random kinetic energy transport equation is written:

$$\begin{aligned}\alpha_p\rho_p\left[\frac{\partial q_p^2}{\partial t} + U_{p,j}\frac{\partial q_p^2}{\partial x_j}\right] = &\\ &- \frac{\partial}{\partial x_j}\left[\alpha_p\rho_p\left(K_p^{kin} + K_p^{col}\right)\frac{\partial q_p^2}{\partial x_j}\right]\\ &- \Sigma^{coll}_{p,ij}\frac{\partial U_{p,i}}{\partial x_j}\\ &- \frac{\alpha_p\rho_p}{\tau^F_{gp}}\left(2q_p^2 - q_{gp}\right)\\ &- \alpha_p\rho_p\frac{1}{3}\frac{1-e_c^2}{\tau_c}q_p^2.\end{aligned} \tag{11}$$

The first term on the right-hand-side represents the transport of the random particle kinetic energy due to the particle agitation and the collisional effects. That term is written by introducing the diffusivity coefficients:

$$\begin{aligned}K_p^{kin} &= \left[\frac{1}{3}q_{gp}\tau^t_{gp} + \frac{2}{3}q_p^2\frac{5}{9}\tau^F_{gp}\left(1 + \alpha_p g_0\zeta_c\right)\right] / \left[1 + \frac{5}{9}\tau^F_{gp}\frac{\xi_c}{\tau_c}\right]\\ K_p^{col} &= \alpha_p g_0(1+e_c)\left[\frac{6}{5}K_p^{kin} + \frac{4}{3}d_p\sqrt{\frac{2}{3}\frac{q_p^2}{\pi}}\right]\\ \zeta_c &= \frac{3}{5}(1+e_c)^2(2e_c-1)\\ \xi_c &= \frac{(1+e_c)(49-33e_c)}{100}.\end{aligned}$$

The second term on the right-hand-side of Eq. (11) represents the production of particle agitation by the gradients of the mean solid velocity. The third term is the interaction with the gas. Finally the fourth term is the particle agitation dissipation by inelastic collisions.